

# Stator Current Spectrum Analysis Applied on Short-Circuit Fault Diagnosis of SRM

**Abstract.** Thanks to power electronics innovation, switched reluctance machine are taking place on industrial applications. In this paper we present the short-circuit fault diagnosis between stator turns of the switched reluctance machine by the use of stator current spectral analysis. To do this, we modeled our switched reluctance machine by permeance networks method to which we have associated the of the teeth contour permeance for the calculation of the airgap. The simulation results show the interest and efficiency of the proposed model as well as the stator current spectral analysis technique for the short circuit fault diagnosis of the switched reluctance machine

**Streszczenie.** W artykule zaprezentowano metodę wykrywania zwarć w silniku reluktancyjnym. Metoda ta bazuje na analizie widmowej prądu stojana. Diagnostyka zwarć w silniku reluktancyjnym bazująca na analizie widmowej prądu stojana

**Keywords:** Switched reluctance machine (SRM), Reluctance network, Short-circuit fault, Stator current, Spectral analysis.

**Słowa kluczowe:** silnik reluktancyjny, diagnostyka zwarć, analiza widmowa.

## Introduction

During the last two decades, power electronics has grown. This allowed to revive the research on the switched reluctance machine (SRM). It exists in different structures whose common property is the significant shape variation of the airgap during the rotation.

In general, the SRM performance can be comparable to that of permanent magnets synchronous machines (PMSM). This machine is robust, inexpensive, reliable in extreme environments [1]. On the other hand, its major defects are the torque ripples and the acoustic noise that they produce.

This machine presents an alternative in multitude applications. It occupies an important place especially for variable drives applications and specific applications such as small pulls, with very satisfactory performance powers that can reach several tens of kilowatts, medical equipment, household appliances, electric vehicles and aerospace fields [2], [3].

SRM is an electromagnetic system involving electrical, magnetic and mechanical quantities. The used methods for the SRM construction were formerly empirical; it was necessary to build the machine, to make tests and measurements and to eliminate one by one the various problems and defects encountered. But it's expensive and takes a lot of time. With the development of computing, design and modeling tools, the cost and time of completion have been greatly reduced. Among these modeling methods we mention the analytical methods; solving the Maxwell equations, semi-numeric methods; such as the reluctance network method and the permeation network method [4], and numerical methods; as an example the finite elements method and finite differences. The choice of method depends on the needs and the application constraints.

Despite their robustness and high reliability, the SRM can have several defects that can impact the mechanical, electrical, control parts or possibly combined defects. It is exposed to various failures such as static and dynamic eccentricity, short-circuit fault between turns and short-circuit between phases, rolling bearing fault, etc. These major failures are due to a variety of causes that are associated with design, manufacture or use. The stator faults and the bearing defects account for nearly 80% of the faults statistics result. For lower power machines, stator faults are less frequent. While the bearing defects and rotor defects are major for high speed machines. Figure 1

Summarized the different faults that can occur in an electric machine. This statistical study is established by reference [5]. This data can be extrapolated also for SRM.

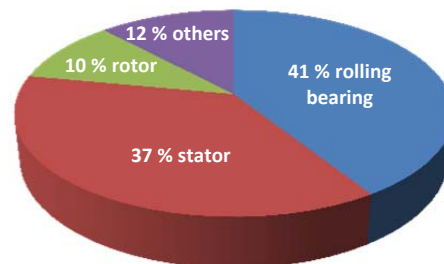


Fig. 1. Statistic study of electrical machine faults and their location

A new algorithm for the real-time diagnosis of power converter faults fed SRM is proposed in paper [6]. The technique shown uses only the measured phase currents.

A 2D finite element analysis of a switched reluctance machine (SRM) under static eccentricity fault is presented in [7]. It describes the influence of the eccentricity on the static characteristics of the motor and shows how to obtain the flow lines and the angular position of the rotor according to both of the healthy and fault conditions.

The main results of the study published in [8] present a new method of diagnosis of eccentricity in a MRV. The method uses 2D finite element analysis to calculate mutual flux and induced voltages in a SRM 8 / 6. Dorrell, D. G., and all describe a study on the rotor eccentricity effects on torque in SRM 8/6 four phases [9].

Differents electrical faults are presented; short-circuit and open-circuit in the SRM in [10].

Different time-frequency methods such as the Wigner-Ville distribution (WVD) and the short-time Fourier transform (STFT) are used in [11] and illustrated for fault detection. The fault detection is important to make a machine diagnosis. Several methods and techniques were developed and implemented. For short-circuit fault detection between turns, several searches are made in [12, 13].

This paper work presents the stator current spectral analysis at the serve of the short circuit fault diagnosis between turns of the SRM. First step, we present a model of nonlinear simulation of SRM based on modeling by reluctance network method associated with the method of the teeth contour for the calculation of the magnetic field in

the airgap. We will then focus on the short-circuit fault analysis between stator turns through the stator current spectral analysis; using FFT Fast Fourier Transformation. Finally, we will present the simulation results of the nonlinear model of the SRM in both of the healthy state and short circuit failure between turns. At the end, a conclusion on the work is done.

### SRM modeling by the reluctances network method (RNM)

#### The SRM 6/4 geometry studied

In this article, our choice was focused on a SRM with 6 stator teethe and 4 rotor teeth, given its geometry simplicity and its power supply.

The stator consists of stacked magnetic sheets having six (6) poles around which are arranged concentric windings. The windings of two diametrically opposed poles are connected in series and form a phase, so we will have three phases for our motor. The rotor meanwhile, has no active element (coil or permanent magnet), and it is also constituted by stacked magnetic sheets having four pole projections Figure 1. Two reference positions are determined for each phase; the opposition position ( $0^\circ$ ) which is the position of misalignment of the axis of the rotor tooth (tooth number 1) relative to the axis of the active stator tooth, and the conjunction position ( $30^\circ$ ) which is the alignment position of the rotor tooth Number 1 with the active stator tooth Figure 2. The successive feeding of the stator phases causes a continuous movement of the rotor.

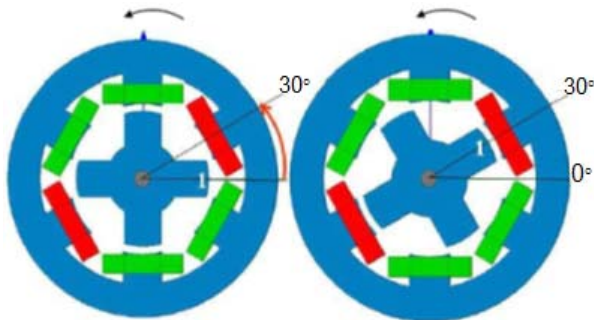


Fig.2. Geometry of 6/4 SRM studied

The converter delivers a voltage across each phase having the following equation below depending on the position of the rotor;  $V$  The constant voltage delivered by the converter,  $\theta_{on}$  the voltage application duration angle,  $\theta_{off}$  the supply end angle and  $\theta_{ext}$  the angle when the current is equal to zero.

$$(1) \quad V(\theta) = \begin{cases} +V & si \quad \theta_{on} \leq \theta \leq \theta_{off} \\ -V & si \quad \theta_{off} \leq \theta \leq \theta_{ext} \end{cases}$$

The voltage inversion is necessary in order to reduce or even cancel the braking torques during the attraction of the rotor by the next coil.

In order to study the dynamic behavior of SRM, the following equations system has strongly non-linear and interdependent elements.

$$(2) \quad \begin{aligned} U_1(\theta) &= R \cdot i_1(\theta) + \omega \cdot \frac{d\phi_1(i_1, i_2, \theta)}{d\theta} \\ U_2(\theta) &= R \cdot i_2(\theta) + \omega \cdot \frac{d\phi_1(i_2, i_3, \theta)}{d\theta} \\ U_3(\theta) &= R \cdot i_3(\theta) + \omega \cdot \frac{d\phi_1(i_3, i_1, \theta)}{d\theta} \end{aligned}$$

where  $U_1(\theta)$ ,  $U_2(\theta)$  and  $U_3(\theta)$  are the applied voltages to the phases 1, 2, 3 respectively.

$R$  is the the winding resistance,  $i_1$ ,  $i_2$  and  $i_3$  are the phase currents.

$\phi_1$ ,  $\phi_2$  and  $\phi_3$  are the main fluxes in the stator poles.  $\omega$  is the rotor speed considered as constant.  $\theta$  is the rotor position.

The resolution of such a system requires an elaborate method that will not only determine the electric current, but also the magnetic flux and position.

The equivalent reluctance network method (RNM) is based on the discretization of the domain to be studied in magnetic zones. These zones are traversed by flux tubes. The reluctance of the flux tube thus becomes a quantity which depends on the magnetic circuit geometry and its permeability. [14]

The SRM study by the RNM makes it possible to represent each zone by a single magnetic reluctance Figure 3.

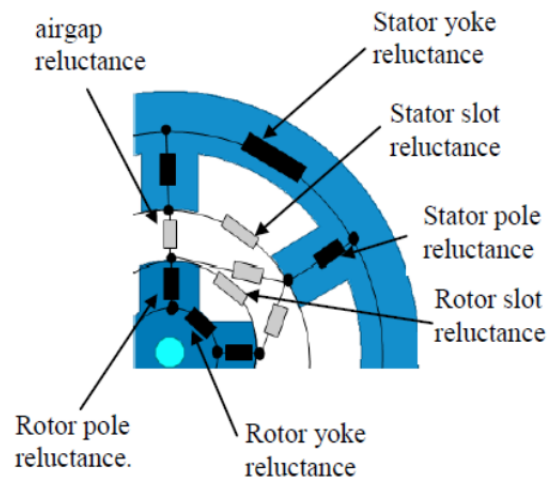


Fig.3. Equivalent reluctances of different magnetic parts of the SRM

The motor's magnetic circuit consists of stator and rotor teeth and yokes. For each part having a length  $L$ , a height  $l$ , and a thickness  $h$ , and taking into account the expansion factor  $k_f$  due to the magnetic sheet lamination, the reluctance will have the form:

$$(3) \quad \mathcal{R}_{mag} = \frac{l}{k_f \cdot \mu \cdot h \cdot L}$$

The stator slot reluctance is given by:

$$(4) \quad \mathcal{R}_{es} = \frac{b_{es moy}}{k_f \cdot \mu_0 \cdot h_{ds} \cdot L}$$

The rotor notch reluctance is given by:

$$(5) \quad \mathcal{R}_{er} = \frac{b_{er moy}}{k_f \cdot \mu_0 \cdot h_{dr} \cdot L}$$

The difficulty of this method is the modeling of the airgap for the consideration of the movement. For that we will use the method of the permutations of the storytellers of the teeth for its adaptability with the RNM.

#### The use of the teeth contour method for the calculation of airgap reluctances

The geometrical shape of the airgap in the double-toothed SRM is complex, which makes it difficult to calculate its reluctances, particularly during the movement of the rotor Figure 4.

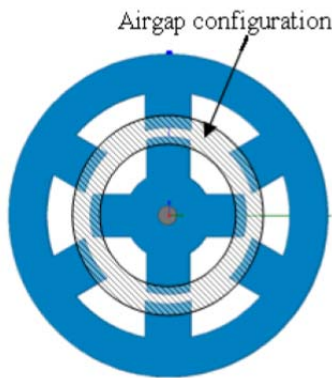


Fig.4. SRM air-gap

In our case, we opted for the teeth contour permeances method for the calculation of the reluctances of the airgap for its adaptability to the method of the equivalent reluctance networks. The calculation of these permeances is done according to the following steps:

- Real curvilinear airgap linearization: To simplify the calculation, we will consider that the airgap is linear Figure 5.

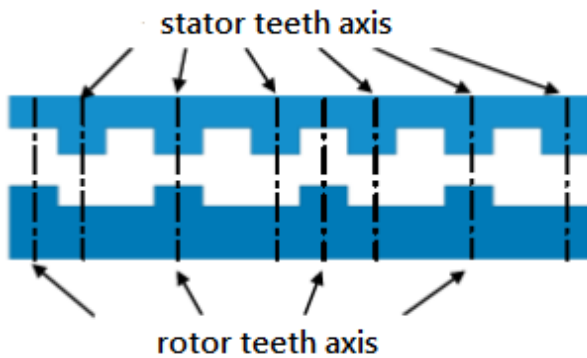


Fig.5. Air-gap linearization according to Carter

- Calculation of the reluctance in the Carter airgap of on a polar step : The airgap is expressed by the following equation

$$(6) \quad e_c = k_{cs} \cdot k_{cr} \cdot e$$

In the following equation,  $e_c$  is the Carter airgap of,  $e$  is the real airgap of the machine and  $k_{cs}$  and  $k_{cr}$  are the Carter coefficients relative to the toothing of the stator and the rotor successively. The Carter permeance under a stator polar step will then be:

$$(7) \quad \mathcal{P}_c = k_f \cdot \mu_0 \cdot L \cdot \frac{T_s}{e_c}$$

- Real notch transformation into a triangular notch : The new airgap will be composed of several forms called overlaps Figure 6

- As shown in Figure 6. we get for a SRM 6/4, 10 overlaps for all rotor positions and therefore 10 airgap reluctances.

The triangle height  $h$  is calculated from the equality between the Carter permeance under a polar pitch and the new triangulated permeance of the airgap expressed as a function of  $h$  as shown in Figure 7.

$$(8) \quad \mathcal{P}_\Delta = \mathcal{P}_c - \mathcal{P}_{em}$$

$\mathcal{P}_{em}$  Is the permeability of the actual smooth magnetic airgap under the tooth.

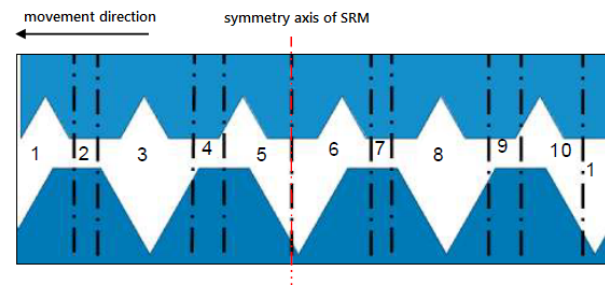


Fig.6. The toothed airgap Triangulation

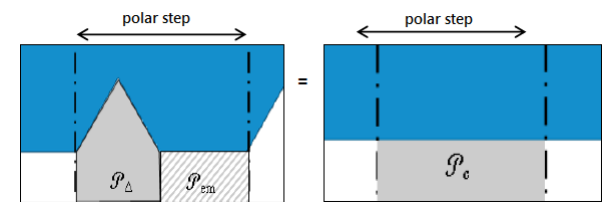


Fig.7. Permeance equality of the triangulated airgap and the Carter airgap

After calculating the permeances of each zone as shown in Figure 6, the total permeance will be:

$$(9) \quad \mathcal{P}_t(\theta) = \mathcal{P}_{e1} + \mathcal{P}_{e2} + \mathcal{P}_{e3} + \mathcal{P}_{e4}$$

Since reluctance is the inverse of permeance, we can write:

$$(10) \quad \mathcal{R}_e(\theta) = \frac{1}{\mathcal{P}_t(\theta)}$$

#### Network reluctance formation of the SRM 6/4

The reluctances of all the magnetic parts thus calculated give us the reluctance network of the SRM 6/4 Figure 8.

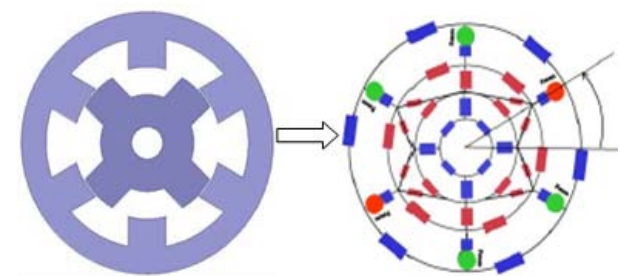


Fig.8. Equivalent reluctance circuit

By writing all meshes equations, we obtain a linear algebraic equations system whose unknowns are flux and currents. In its matrix form, the equations system of will be written in matrix form:

$$(11) \quad [\mathbf{F}] = [\mathbf{R}] \cdot [\boldsymbol{\varphi}]$$

Where  $[\mathbf{F}]$  is the magnetomotive forces matrix,  $[\mathbf{R}]$  is the reluctances matrix of the magnetic circuit and  $[\boldsymbol{\varphi}]$  is the flux matrix flowing in the meshes.

The preceding equations system is a linear algebraic system. For its resolution several methods are available. Among them, the Euler method, it is a simple method, easy to implement, having a fast convergence and a good precision. The resolution of this system makes it possible to calculate the main flux necessary for the resolution of the

SRM differential equations and the determination of the phase current.

In the following, the overall calculation algorithm is depicted by the following flowchart:

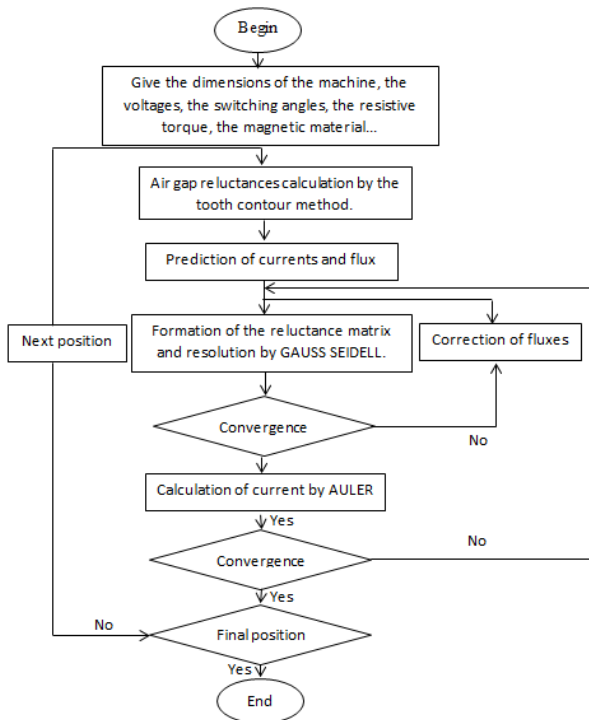


Fig.9. Resolution flowchart of the system of equations representing the SRM

### Integration of short-circuit fault between turns

The SRM modeling and simulation under short-circuit failure between turns are an important steps for the detection of this type of fault and its diagnosis, because it is difficult, even theoretically, to include all the imperfections that exist in the machine in a fault case.

In this case, we will first analyzing the stator current corresponding to the faulty phase, because it provides accessible information outside of the machine.

A short circuit between turns is a fairly common fault. It is originate from one or more insulation defects in the concerned winding. It causes a stator current increase in the faulty phase.

To apply a short-circuit fault in a non-linear regime, it is necessary to reduce the turns number and consequently a decrease in the stator slot reluctance. In the healthy state the turns number  $N$  of the studied machine is 100 turns. At the application instant of a 10% short-circuit fault between turns, the turns number is reduced to 90 turns corresponding to the faulty phase. It should be noted that the magnetomotive force expressions, torque and flux are given as a function of  $N$ .

### Monitoring through statoric currents analysis

Faults that can occur on electrical machines have a direct impact on the frequency content of the stator or rotor currents [15, 16].

The extraction of the information contained in the discrete signals concerning the fault requires the passage of the time domain towards the frequency domain. The Fast Fourier Transform (FFT) is one of the tools used in the case of stationary signals (steady-state machines, faults impacting constant frequency components over time).

The spectral analysis monitoring of the variable reluctance machine therefore consists in performing a Fourier transform of the quantities affected by the fault, and in displaying the parasitic frequencies constituting the fault signature in the machine [17]. The chosen quantities are electrical (more particularly the stator current). This technique allows a quick and inexpensive monitoring because it requires simple current sensors.

### Simulation results

First we chose a basic SRM with the mentioned dimensions in the appendix.

In the following figures, we give the main simulations results relating to different windings conditions (current in the healthy case and with short circuit fault between turns of 10% as a function of time).

The traited quantities in the simulations are the stator current and the magnetic induction. In order to see the fault impact on the machine, a spectral analysis of these last two quantities is necessary. Therefore, we present the stator current temporal shape and its spectral form and the magnetic induction. All simulations were performed at the imposed constant speed of 1500 rpm, 60 volts voltage and the resistance is 2.30 ohm.

The simulations are done by reluctance network method using Matlab software for numerical simulation.

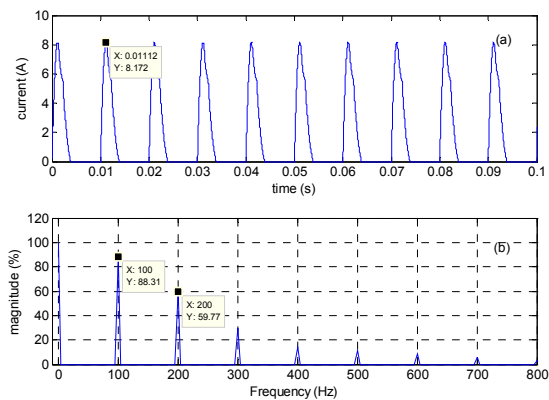


Fig.10. Stator current in the healthy operating case, a: time domain, b: spectral domain

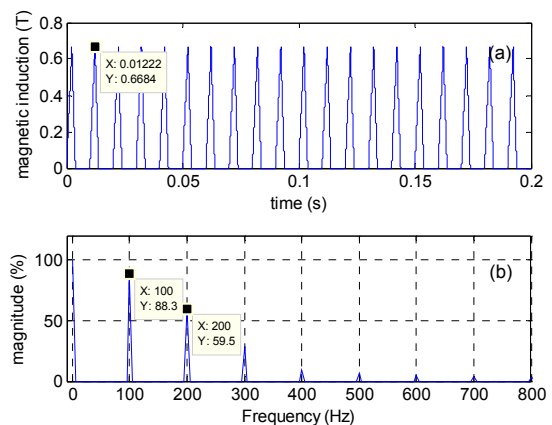


Fig.11. Magnetic induction in the healthy operating case, a: time domain, b: spectral domain

### Healthy machine

Figure 10 represent the stator current temporal shape (1a) and its spectral form in healthy state machine case. The current increases to a maximum value of 8.172 A,

decreases and becomes, then increases again. The stator current contains the fundamental harmonic and their multiples.

The Figure 11 shows the shapes of the stator magnetic induction of the machine as a function of time. The induction increases to a maximum value of 0.668 T, then decreases and becomes zero, and after a while it resumes growth (as in the case of the current).

### Machine with 10% between turns short-circuit fault

Figure 12 and Figure 13 respectively represents the temporal shape of the stator current, the magnetic induction and its spectral form in the case of an operation under a 10% short-circuit fault.

In case of 10% short circuit between turns, if we compare the current and the magnetic induction corresponding to the faulty phase with the healthy case; it is clearly seen that the current increases from 8.172 A to 11.63A and from 0.668T to 0.77T for the magnetic induction. The case of a short-circuit between turns does not give new harmonics. On the other hand a clear increase of the amplitude of multiple harmonics of the fundamental one is observed. The amplitude variation is more significant and visibly clear for the 100Hz 200Hz and 300Hz frequencies.

The obtained results by the reluctance network model correspond with a very good precision and very short time computing.

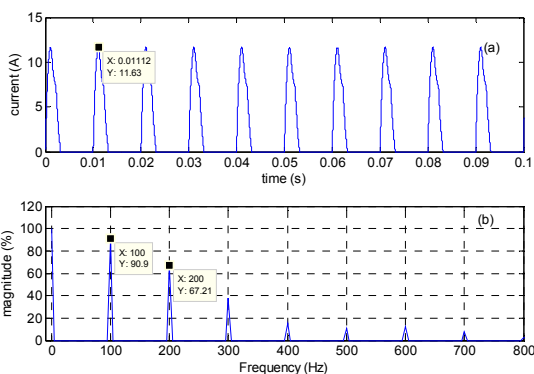


Fig.12. Stator current in the faulty operating case (Short-circuit fault), a: time domain, b: spectral domain

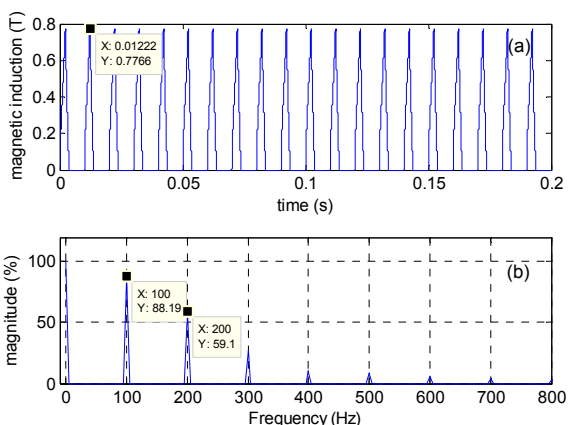


Fig.13. Magnetic induction in the faulty operating case (Short-circuit fault), a: time domain, b: spectral domain

### Conclusion

The presented paper work addresses the short-circuit fault diagnosis of between stator turns for the SRM by the use of stator current spectral analysis. At first, we presented a state of the art on the SRM. This type of machine is especially appreciated for its simplicity and robustness as well as its low cost for very interesting performances. In a second step, we have established a 2D model of SRM based on the reluctance network method associated with the teeth contour method for the calculation of the magnetic field in the airgap. Our model has proved reliable and accurate with a reduced calculation time. Stator current Spectral analysis has shown that the short-circuit fault is manifested by the amplitude increase of the fundamental multiple rays.

### Appendix

Table 1, VRM dimensions

Dimensions (mm)	Stator	Rotor
Inner diameter	47	5
Outer diameter	81	46
Teeth height	10	10
Teeth width	10	16
Yoke thickness	10	9
number of poles	6	4
length	150	150
air-gap	0.5	

### Authors:

Phd student. Rabeih Chehda Diagnostic Group, LDEE laboratory, Electrical Engineering faculty, University of Science and Technology of Oran MB, BP 1505 El-Mnaouer Oran 31000, Algeria, E-mail: [rabeih.chehda@univ-usto.dz](mailto:rabeih.chehda@univ-usto.dz)

Prof. Noureddine Benouzza Diagnostic Group, LDEE laboratory, Electrical Engineering faculty, University of Science and Technology of Oran MB, BP 1505 El-Mnaouer Oran 31000, Algeria, E-mail: [benouzza@yahoo.com](mailto:benouzza@yahoo.com)

dr. Naouel Kada Belghitri Diagnostic Group, LDEE laboratory, Electrical Engineering faculty, University of Science and Technology of Oran MB, BP 1505 El-Mnaouer Oran 31000, Algeria, E-mail: [kabelnaw@yahoo.fr](mailto:kabelnaw@yahoo.fr)

### REFERENCES

- [1] Zhu, Z. Q., Howe, D. "Electrical Machines and Drives for Electric, Hybrid, and Fuel Cell Vehicles", Proceedings of the IEEE, 95(4), pp.746–765, 2017. <https://doi.org/10.1109/jproc.2006.892482>
- [2] Sadeghi, S., Mirsalim, M. "Dynamic Modeling and Simulation of a Switched reluctance Motor in a Series Hybrid Electric Vehicle", Acta Polytechnica Hungarica, 7(1), pp. 51-71, 2010.
- [3] Mahmoud, I., Rehaoulia, H., Ayadi, M. "Design and modeling of a linear switched reluctance actuator for biomedical applications", International Journal Of Physical Sciences, 6(22), pp. 5171-5180, October 2011.
- [4] Kada Belghitri, N., Taieb Brahimi, A., Kernane C. "using reluctance network method in SRM design", In: Proceeding of international conference on electrotechnics ICCEL2013, Oran, Algeria, December 2013, pp. 10-11.
- [5] Deekshit, K.C., Venu Gopala Rao, M., Srinivasa Rao, R. "DWT based bearing fault detection in induction motor using noisecancellation", Journal of Electrical Systems and Information Technology, 3 (3), pp. 411–427, December 2016.
- [6] Marques, J. F., Estima, J. O., Gameiro, N. S., Cardoso, A. J. M. "A new diagnostic technique for real-time diagnosis of power converter faults in Switched reluctance motor drives", IEEE Transactions on Industry Applications, 50(3), pp. 1854-1860, May-Jun. 2014.
- [7] Faiz, J., Pakdelian, S. "Finite-element analysis of a switched reluctance motor under static eccentricity fault", IEEE Trans. Magn., 42(8), pp. 2004-2008, Aug. 2006.
- [8] Faiz J., Pakdelian, S. "Diagnosis of static eccentricity in switched reluctance motors based on mutually induced voltages", IEEE Transactions on Magnetics, 44(8), pp. 2029-2034, Aug. 2008.

- [9] Dorrell, D. G., Chindurza, I., Cossar, C. "Effects of rotor eccentricity on torque in switched reluctance machines", IEEE Transactions on Magnetics, 41(10), pp. 3961-3963, Oct. 2005.
- [10] Gopalakrishnan, S., Omekanda, A. M., Lequesne, B. "Classification and remediation of electrical faults in the switched reluctance drive", IEEE Transactions on Industry Applications, 42(2), pp.479-486, Mar.-Apr. 2006.
- [11] Bouchareb, I., Bentounsi, A., Lebaroud, A., Batoun, B. "Dynamic Eccentricity Fault Detection In Switched Reluctance Motor Using Time-Frequency Analysis", In: 6th International conference on Sciences of Electronics, Technologies of Information and Telecommunication SETIT 2012, Tunisia, March 2012, pp. 21-24.
- [12] Bouchareb, I., Bentounsi, A., Lebaroud, A. "An Integrated Artificial Neural Networks/Optimal Time-Frequency Based Classification in Condition Monitoring of Synchronous Reluctance Motor Stator Fault" 9th IEEE International Symposium on Diagnostics for Electrical Machines, Power Electronics & Drives SDEMPED 2013, 27-30 August 2013, Spain.
- [13] Bouchareb, I., Bentounsi, A., Lebaroud, A. "Advanced Diagnosis Strategy for Incipient Stator Faults in Synchronous Reluctance Motor", In: IEEE 10th International Symposium on Diagnostics for Electrical Machines, Power Electronics and Drives (SDEMPED), Guarda, Portugal, 2015, pp. 110-116.
- [14] Bekkouche, B., Chaouch, A., Mezari, Y. "A Switched Reluctance Motors Analyse using Permeance Network Method", International Journal of Applied Engineering Research, 1(2), pp. 137-152, 2006.
- [15] Benbouzid, M.E.H. "A review of induction motors signature analysis as a medium for faults detection", IEEE Transactions on Industrial Electronics, 47(5), pp. 984-993, October 2000.
- [16] Elbouchikhi, E., Choqueuse, V., Benbouzid, M. "Induction machine diagnosis using stator current advanced signal processing", International Journal on Energy Conversion, 3(3), pp. 76-87, May 2015.
- [17] Harir, M and Bendiabdellah, A. " Stator Current Spectral content of an Induction Motor taking into account Saturation Effect", Przegląd Elektrotechniczny, 11, pp.108, 2018.
- [18] doi:10.15199/48.2018.11.25